GEOLOGICA CARPATHICA, 54, 3, BRATISLAVA, JUNE 2003
153–162

RELATIONSHIPS BETWEEN FOLDING AND FRACTURING IN OROGENIC BELTS: EXAMPLES FROM THE RHENOHERCYNIAN ZONE (GERMANY) AND THE EXTERNAL HELLENIDES (GREECE)

SOTIRIOS KOKKALAS, PARASKEVAS XYPOLIAS, IOANNIS K. KOUKOUVELAS*, and THEODOR DOUTSOS

Department of Geology, University of Patras, 26500 Patras, Greece; *iannis@upatras.gr

(Manuscript received April 30, 2002; accepted in revised form December 12, 2002)

Abstract: The kinematic similarities of small-scale structures in the Rhenohercynian Zone and the external zones of the Hellenides are illustrated. Both orogenic domains comprise asymmetric folds verging toward the foreland and are affected by extensional joints (*ac* and *bc*) associated with hybrid joints as well as with shear fractures ($hk0_a$ and $hk0_b$). Joints were formed during layer bending which took place throughout the fold evolution and were symmetrically arranged with respect to principal stresses σ_1, σ_2 and σ_3. Although the magnitude of the stress axes changed during folding, their orientation with respect to layering remained constant: one of them is orientated perpendicular to the layering, whereas the other two are parallel and perpendicular to the dip direction of the layering respectively. As expressed by *ac* and hybrid joints the extension normal to the dip direction of layering progressively increased during fold tightening. Layer parallel shear responsible for the asymmetry of the folds caused joint rotation toward the fold hinge within the long limb. Furthermore, these movements controlled at both limbs the formation of *bc* and associated hybrid joints during the folding.

Key words: Rhenohercynian, Hellenides, folding, extensional joints, hybrid joints, shear fractures.

Introduction

Complexities in the analysis of small-scale structures in fold-and-thrust belts are produced due to the coexistence of extensional, compressional and wrench structures, each one close to the other. This coexistence appears to give conflicting information regarding the stress system during folding (see also Price & Cosgrove 1990).

Small-scale structures have long been used to delineate the temporal progression of deformation. We use the term small-scale structures to cover small faults, small folds, stylolites, cleavage, shear-zones, veins and joints. From these small-scale structures, the fractures that include joints and small faults are the most important for understanding fluid circulation and mineral precipitation within rocks and have been analyzed in this contribution. Adopting the nomenclature of Dennis (1972), Hancock (1985) and Price & Cosgrove (1990), fractures that range in size from centimeters to tens of meters can be divided into three groups (Fig. 1): (a) Dilation fractures or Mode I cracks characterized by open space with or without mineral precipitation. (b) Shear fractures bearing horizontal slickenlines and (c) oblique extension fractures or hybrids characterized by oblique slip as well as fractures of intermediate type. The attitude of fractures related to folds are described with respect to three orthogonal reference axes in three different ways: (a) *The layer-control system* (Price 1967; Stearns 1967), in which the three reference axes are oriented parallel to layer strike, layer dip and normal to layering. (b) *The layer- and the fold-control system* as introduced by Price (1967) and Hancock (1985), in which the reference axes are parallel to the fold axis, parallel to the layering and normal to the fold axis, and normal to layering (Fig. 1A). (c) *The fold-control system* (Hobbs et al. 1976), in which the axes are parallel to the fold axis, parallel to the axial surface and normal to the fold axis, and normal to the axial surface. Note that most of these classifications were used to describe fractures related to symmetrical folds.

Natural examples and mechanical analyses in fold-and-thrust belts have documented that fold asymmetry due to simple shear is common during fold development (Sanderson 1979). In addition flexural-slip mechanism is important through fold evolution and accompanied by slip along “competent units” (Chester et al. 1991; Gray & Mitra 1993; Tanner 1989; Ohlmacher & Aydin 1995, 1997; Cooke & Pollard 1997; Couples et al. 1998). Competent units are defined by surfaces that host slip (see also Couples et al. 1998) and can include one thick and massive bed or a series of beds showing similar mechanical behavior.

Studies relating folding to stages of fracturing indicate that jointing appears to develop under the influence of fluid pressure and temperature (i.e., Skarmenta & Price 1984; Srivastava & Engelder 1990; Gray & Mitra 1993).

In this paper, we present data pertaining to the orientation and kinematics of fractures developed during folding by tangential longitudinal strain. In this process extension or stretching acts all along the outer arc of the folds tangentially, while compression acts along the inner arc. It is shown that the fracture network in short and long limbs of the asymmetric folds can be divided into bending related fracture assemblages which were strongly affected by an imposed shear. Shear

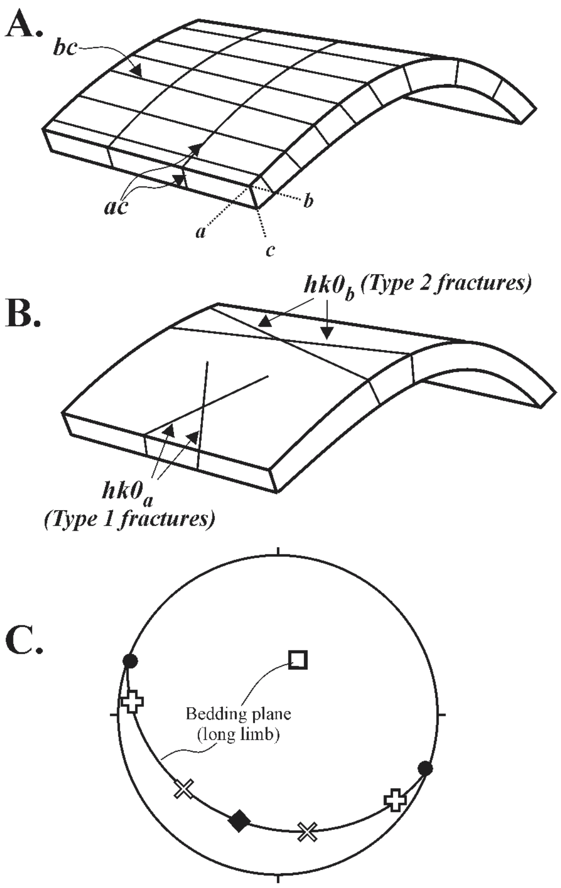

	after STEARNS 1967	after HANCOCK 1985
●	—	*ac*
◆	—	*bc*
✚	*Type 1 fractures*	$hk0_a$ fractures enclosing an acute angle about *a*
✖	*Type 2 fractures*	$hk0_b$ fractures enclosing an acute angle about b

Fig. 1. Relationships of (**A**) dilational and (**B**) shear fractures with a fold. Fabric axes following the *layer-* and the *fold-control system*. (**C**) Ideal relationships of *ac*, *bc*, $hk0_a$ and $hk0_b$ fractures to a stereonet. Legend for explanation of symbols in the ideal stereonet and to show nomenclature after Stearns (1967) and Hancock (1985), for more explanations see text.

strain in fold-and-thrust belts can be generated during the overthrust of the internal parts of the orogen onto the underplated external parts (i.e., Gray & Mitra 1993) along crustal scale shear zones. Two regions, the Rhenohercynian Zone of the Variscan orogenic belt (Germany) (Figs. 2, 3 and 4) and the external Hellenides of the Alpine orogenic belt (Greece) (Figs. 5, 6 and 7) are studied.

Methodology

The analysed stations were selected where the enveloping surfaces of folds can be recognized and this enables reliable identification of the short and long limbs of folds. Then orientation data were collected in the stations using the "selection method" (Davis 1984), wherein sets of fractures are visually determined and three to seven orientations are measured on each fold limb; 25 measurements were the minimum for a station, unless the exposure was limited. The selection method is commonly used in study of fractures (i.e., Hancock 1985; Engelder & Geiser 1980; Dunne 1986). The stations were classified into domains by limb dip (0–30°, 30–60°, 60–90° and overturned) (Dunne 1986). The second step of data collection includes mesoscopic descriptions of the small-scale structures, the dihedral angles between sets of conjugate fractures, the overprinting relationships between fractures, the types and attitude of vein fills, the attitudes of stylolites, evidence for displacement along joint surfaces, the amount of movement along slip surface and the direction of slickensides. In the final step of data collection, thickness of beds, slickensides of bedding planes, small-scale folds, duplexes developed on the bedding planes, and attitude of normal and thrust faults which cut one or more beds or mechanical units were measured. The collected data were plotted on four equal area nets following the limb dip classification into four domains, three of them for the long limb and one for the short limb. For the consideration of fracture distribution in the equal area nets we follow the methodology by Dunne & Hancock (1994). Analytically, we recognize the occurrence of single sets of fractures and sets of fractures displaying dispersion about the mean orientation on these stereonets. As a single set we recognize a maximum with dispersion less than 10°, while maxima reflecting the presence of two sets display dispersion of >10°. Finally, when the 2θ angles between the sets range between 10 to 50° this dispersion corresponds to hybrid joints, while 2θ angles ranging between 60–90° correspond to shear fractures.

The case of the Rhenohercynian Zone

The geology of the Rhenohercynian Zone

The Rhenohercynian Zone represents a Devonian to Lower Carboniferous passive continental margin accumulating 3–12 km thick marine clastics and carbonates (Meyer & Stets 1980). The southern parts of this margin comprise telescoped slope and rise sequences bordering a small oceanic basin between the Rhenohercynian and Saxothuringian Zones (Fig. 2) (Dittmar & Oncken 1992). Contractional movements started during the earliest Late Devonian, resulted in a SE-directed subduction causing the consumption of the intervening oceanic basin as indicated by the onset of flysch sedimentation and the evolution of a magmatic arc in the south on the Mid-German crystalline rise (Plesch & Oncken 1999). The orogenic front propagated from south to the north from ca. 325 Ma to 300 Ma, causing the formation of NW-verging map scale synclines and anticlines (Wunderlich 1964; Ahrendt et al. 1983). Major thrusts, producing antiformal stack-type structures at depth are rooted in a crustal scale decollement at a depth of 13–16 km (Oncken 1998). Internal deformation within the Rhenohercynian Zone is controlled by the flexural-slip mechanism (Fig. 4) associated with frictional sliding and pressure so-

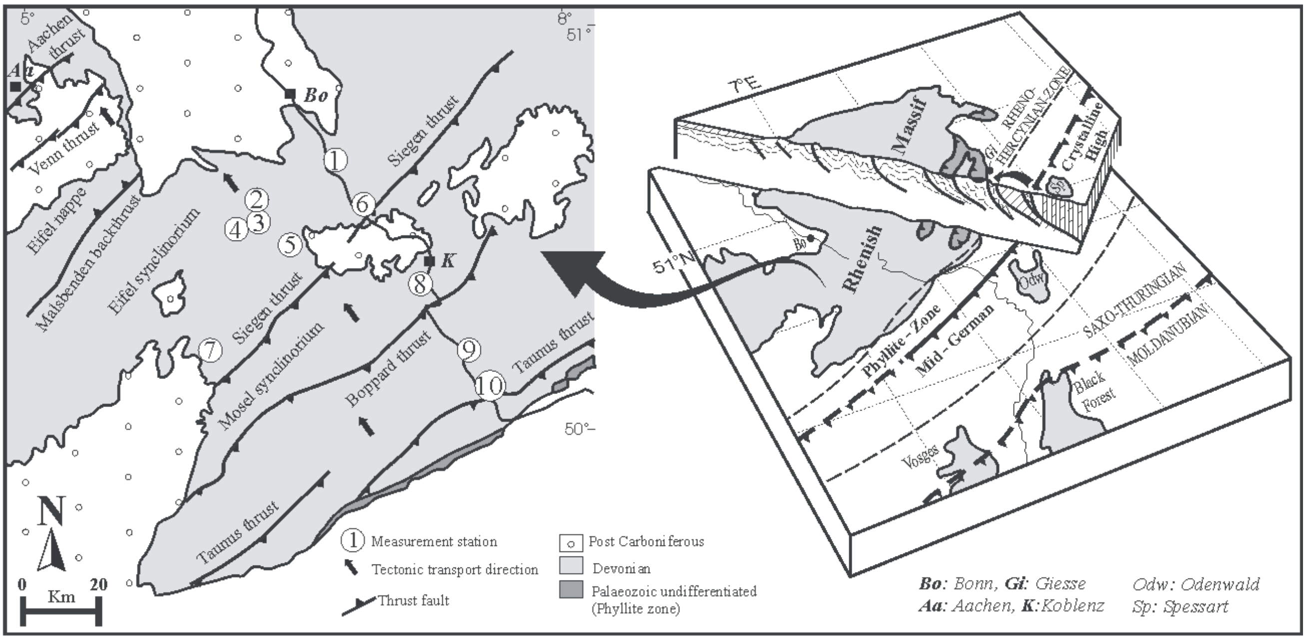

Fig. 2. Simplified geological map of the Rhenohercynian Zone showing major thrusts and transport direction (after Meyer & Stets 1980) and interpretative block diagram of the main Variscan structures in Central Europe (modified, after Martin & Franke 1985).

lution (Cloos & Martin 1932; Breddin 1956; Plessmann 1966). Pressure-temperature metamorphic conditions are higher to the south (estimated P≈6 kbar and T≈350 °C) (Meisl 1990) and decrease toward the north (Fig. 2). Metamorphism is estimated at the anchizone conditions below the Siegen Thrust (Meyer et al. 1986).

Long limb deformation

In order to refine symmetrical relationships between fractures and bedding orientation we summarize fracture data collected in places where the bedding attitude is nearly horizontal, moderately and steeply dipping.

Common fractures affecting the nearly horizontal long limbs are represented by a set of NE-trending and NW- or SE-steeply dipping joints that are classified as *bc* joints (Fig. 3, nets A1 and A2). Irregular fracture planes, and typical absence of slickensides as well as little or no offset along the bedding plane characterize these joints. However, in case the attitude of the fractures is more than 10° of the mean orientation, the *bc* joints display oblique slickensides. Thus we interpret joints with attitude dispersion of less than 10° as tension or Mode I cracks, while fractures with a large dispersion in the NW- and SE-quadrant (Fig. 3, nets A1 and A2) are regarded as hybrid *bc* characterized by oblique extension. The opening of joints ranges between 0.5–1.5 cm and in some cases they have quartz filling. A NW-trending joint set dipping steeply either to the NE or to the SW is typical for almost all horizontal long limbs, those sets following the layers are classified as *ac* joints. The kinematics as well as the attitude of this joint set is similar to the *bc* joints showing a scatter over the sectors of the equal area net (Fig. 3, nets A1 and A2) and thus this set includes tension, as well as hybrid fractures which are characterized by oblique extension.

The fracture network affecting the moderately inclined long limbs is similar to the networks appearing on the nearly horizontal limbs. Sets of fractures recognized on these limbs are classified as *ac*, *bc* and hybrids of these two sets. However, on these limbs two additional conjugate fracture systems were recognized, which form an acute angle about the *a* and *b* reference axes (Figs. 1B, 3; nets B1 and B2), respectively. Mesoscopic structural analysis of these fractures indicates that most of them are characterized by horizontal slickensides and thus they are classified as shear fractures. Additional extension in these limbs is represented by planar NW-facing normal faults (Fig. 3, net B2: N_1 and N_2) displaying small dip-slip displacements. The sense of slip is defined by the displacement of marker beds in the schist. Moreover, a series of en-echelon planar or sigmoidal veins showing oblique slip kinematics are developed, in respect with these normal faults, which are classified as oblique extensional fractures. Offset on these oblique slip faults range from a few centimeters to 5 m and their lengths may exceed 50 m with the possibility of much longer dimensions along strike in the Altenburg-Altenahr area (Fig. 2, Measurement stations 1 to 4).

Steeply dipping limbs are affected by all previous described fractures with the $hk0_a$ shear fractures as the most prominent (Fig. 3, net C1 and C2). Another joint maximum at the SW quadrant of the equal area net C1 in the Fig. 3 cannot be classified according to the *layer- and the fold-controlled system* and may be attributed to post orogenic movements of the area. Shortening is controlled by SE-dipping reverse faults (Fig. 3, net C2: T_1 and Fig. 4A and B) in similar orientation with previously analysed normal faults.

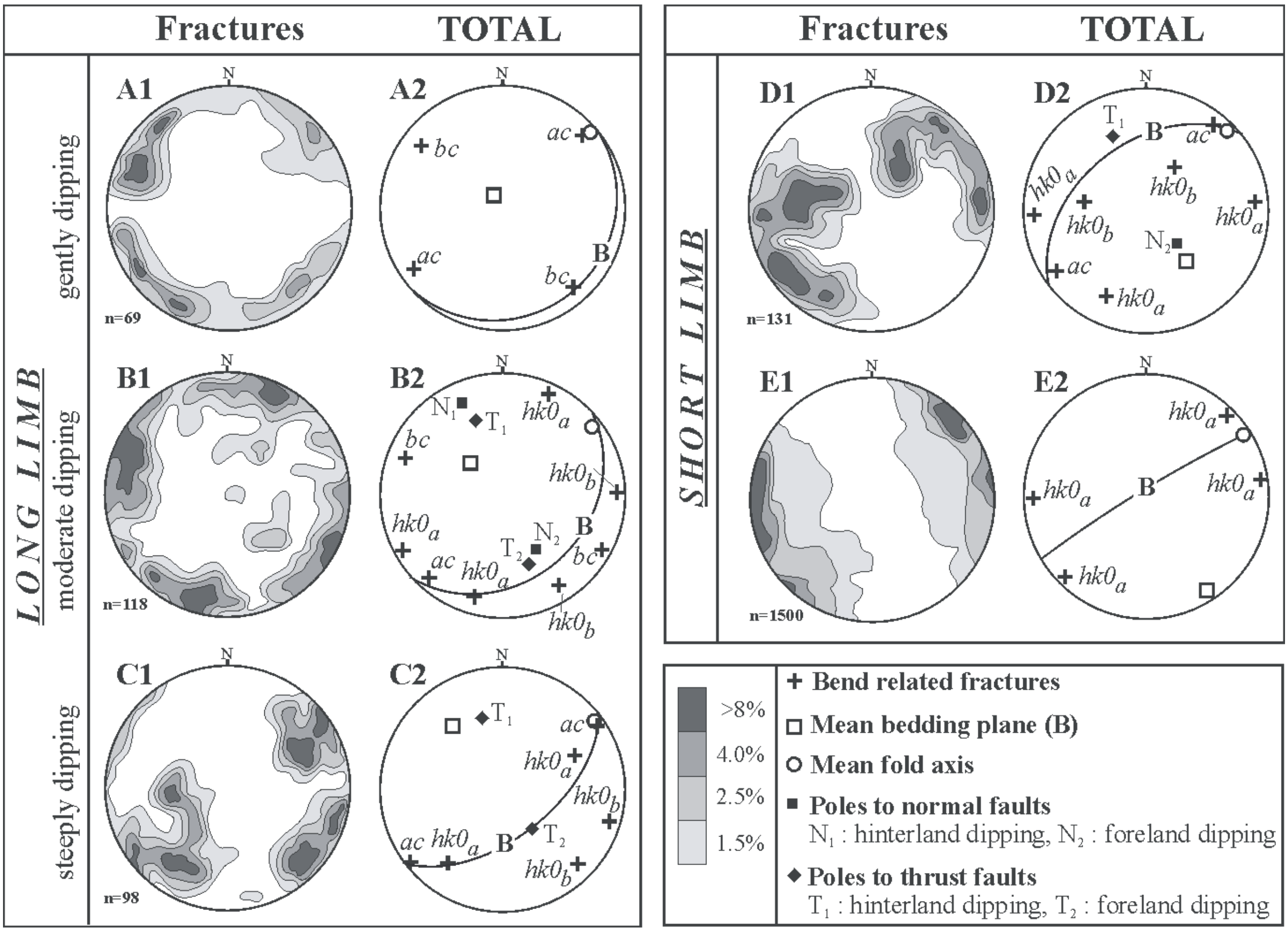

Fig. 3. Equal area lower hemisphere projections illustrating clustering of mesofracture in the Rhenohercynian Zone. Nets (**A1**) to (**C1**) correspond to long limbs, and nets (**D1**) and (**E1**) correspond to short limbs. Data in equal area net (**E1**) comes from the Taunus area (modified, after Doutsos & Prufert 1986). Equal area nets (**A2**) and (**E2**) show labelling of clusters in respect to the mean bedding plane (**B**) and following Hancock's (1985) classification. For details see text.

The distribution of shear fractures belonging to $hk0_a$ and $hk0_b$ forms an acute angle with the bedding reaching up to 30^o (Fig. 3, nets B1, B2 and C1, C2). This can be explained by forward rotation of formed fractures during layer parallel slip (see Synthesis).

Short limb deformation

The short limb was affected by *ac*, $hk0_a$ and $hk0_b$ fractures (Fig. 3, nets D1, D2, E1 and E2). Bedding perpendicular veins allied with *hk0* shear fractures are common and are often displaced by bedding parallel shear (Fig. 4C). In the Taunus at the southern parts of the Rhenohercynian Zone, where the short limbs belong to upright isoclinal fold, $hk0_a$ joints prevail (Fig. 3, E2, Doutsos & Prufert 1986). Limb shortening is expressed by wedge folds (sensu Cloos 1961), layer parallel slip, top-to-NW small scale thrust faults, continuous and disjunctive cleavage and kink bands.

Thrusts cutting up from the base to the top of competent sandstone layers illustrate the early stage of ramp-related folding or wedge folding and imply thickening of layers where layers were sub-horizontal. Subsequently bedding was rapidly steepened to a nearly vertical position and then the short limb extended by gently SE-dipping and NE-trending small-scale thrust faults that cut the beds (Fig. 3, net D2: N_2 and T_1). These minor thrusts, which were formed after the steepening of the short limb, essentially accommodate distributed shear away from the major thrust planes.

The case of the external Hellenides

The geology of the external Hellenides

The Apulia platform in the external Hellenides represents a Mesozoic passive continental margin comprising a 2–4 km thick sequence of calcareous rocks, evaporites and cherts (Bernoulli & Laubscher 1972) (Fig. 5). During the Late Jurassic, this margin was subdivided by rifting into two shallow-water platform areas namely the Tripolitsa and the pre-Apulia Zones, which were separated by the deep-water Ionian Basin (Auboin 1959; Karakitsios 1995). To the east the Apulian margin was thinned and passed gradually into a thin pelagic sequence of cherty limestones and radiolarites known as "the

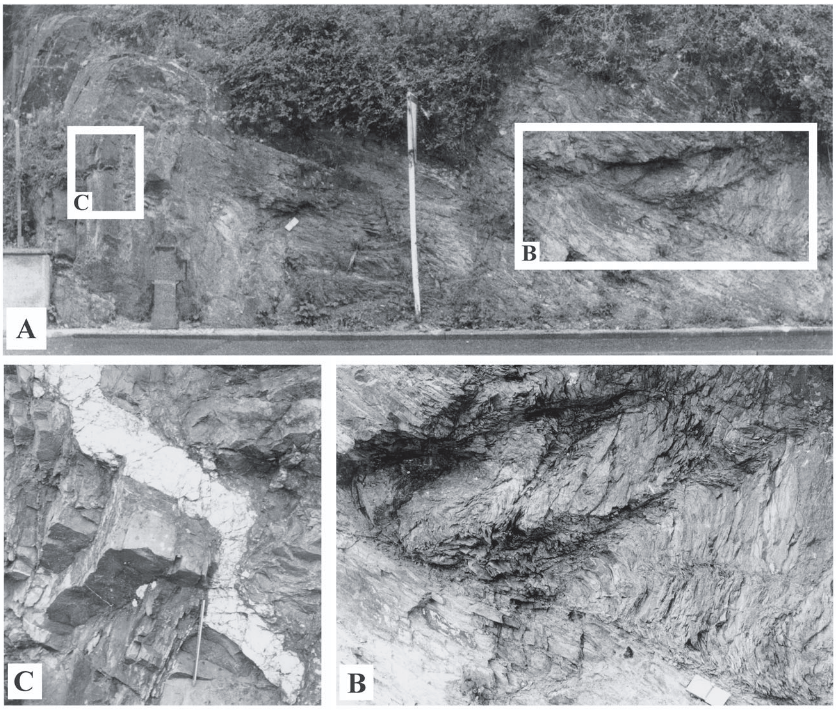

Fig. 4. The asymmetrical Schuld fold at Altenahr-Kreuzberg location, first described by H. Cloos, in Lower Devonian schists. (**A**) General view, photo was taken looking SE. (**B**) Detail of the long limb (the right part of the photo A) deformed by normal faults, compass for scale. (**C**) Detail of the short limb to the left of the monument, the photo shows layer slip expressed by the offset of a quartz vein, pencil for scale.

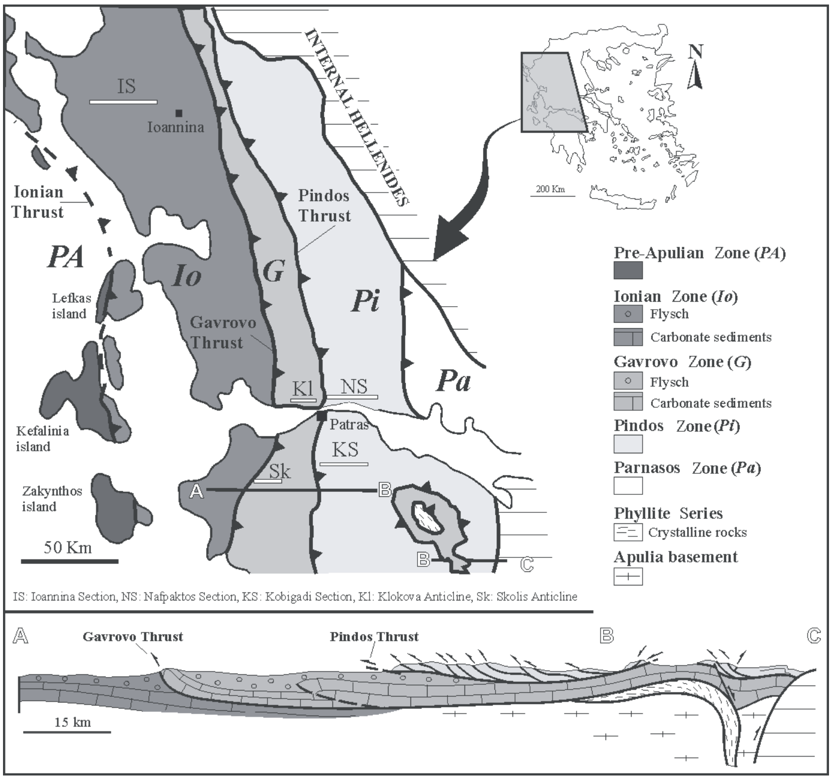

Fig. 5. Simplified geological map and cross-section (modified, after Xypolias & Doutsos 2000) of the external Hellenides showing isopic zones, major thrusts, and analysed cross-sections. Inset shows the location of the study area in the Greek Peninsula.

Pindos zone" which bordered the Pindos Ocean (Smith et al. 1979; Degnan & Robertson 1998) (Fig. 5). In the Late Eocene plate convergence commenced and the Pindos Ocean subducted eastwards below the Pelagonian microcontinent (Fig. 5) (Temple 1968; Pe-Piper & Koukouvelas 1992; Doutsos et al. 1993, 2000; Xypolias & Koukouvelas 2001). The Pindos Zone was separated from its basement and was highly deformed into a series of imbricate thrust sheets that were finally emplaced over the Tripolitsa Zone to the west (Xypolias & Doutsos 2000). As a result the Apulian margin was thickened, uplifted and subdivided into synorogenic flysch basins, which were formed during the southwestward propagation of thrusting and folding until the Middle Miocene time (Richter 1978). Internal deformation in the Apulian platform occurred under nonmetamorphic conditions at burial depths not greater than 5 km (Kisch 1981). This deformation was predominantly achieved by pressure solution and fracturing (Xypolias & Doutsos 2000) (Fig. 7).

Long limb deformation

In the initial stages of folding, fold long-limbs have dips between 5–30° and are affected by *bc*- and *ac*-joints as well as $hk0_a$ joints (Fig. 6, net A1 and A2). The cluster in the north sector of the net corresponds to a complex double cluster including *ac* joint and hybrid *ac* joints and $hk0_a$. Similarly, most of the clusters appeared in the net A1 display dispersion more than 10° about the mean orientation and thus we infer that hybrid fractures are widespread during this stage.

In many places stylolites perpendicular to the bedding plane indicate contraction of bedding parallel to the dip direction. In other places, and especially where the fold limbs dip at 20–30°, stylolites are widened to become bed-normal calcite-filled veins (Fig. 7a). In addition stratal extension and limb thinning are accommodated by normal faults. Normal faults form a conjugate NNW-trending set with dominant ENE-dipping faults (Fig. 6, net A2: N_1 and N_2). Those faults have small displacements (1 cm to 1 m), and most of these are confined in the competent units. Normal faults, duplexes and small folds in weak beds suggest accommodation to the westward nappe transportation and therefore are clas-

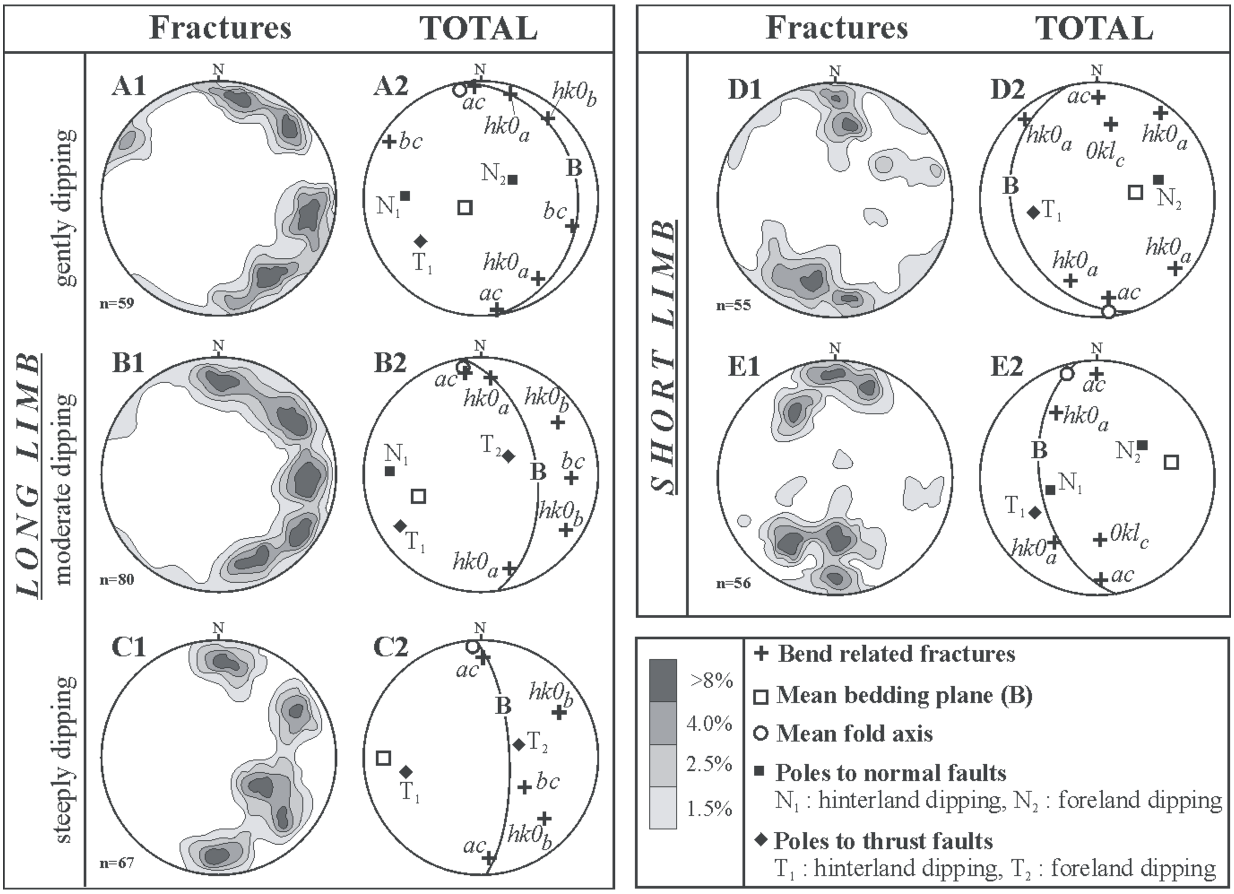

Fig. 6. Equal area lower hemisphere projections of structural data from representative stations in external Hellenides. Nets (**A1**) to (**C1**) illustrate clustering of fractures in long limbs with respect to sedimentary layering and fold hinge lines, nets (**D1**) and (**E1**) illustrate clustering of fractures in short limbs from representative stations and the Klokova Anticline respectively. The equal area nets (**A2**) to (**E2**) show labelling of fracture clusters to long and short fold limbs, nomenclature as in Fig. 3.

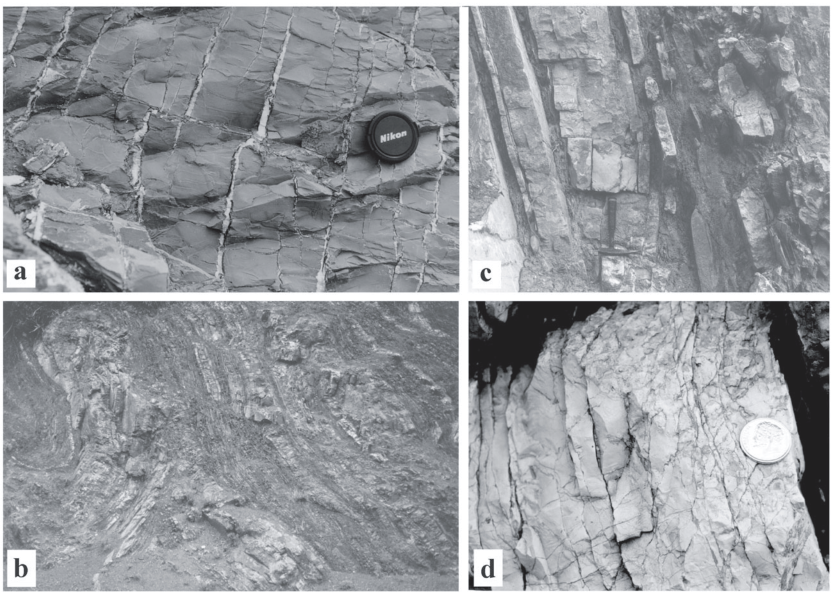

Fig. 7. Key structural observations in the Pindos Zone. (**a**) Stylolites perpendicular to the bedding widened to calcite veins, lens cap for scale. (**b**) A lift-off fold affected by east dipping out-of sequence thrusts, field of view is 20 m. (**c**) A series of east dipping small scale thrust faults affecting a steeply dipping long limb, hammer for scale. (**d**) Sub-vertical stylolitic cleavage affecting the inverted fold limb, coin for scale. Photos (a) to (c) were taken looking north while photo (d) was taken looking south.

sified as transport related small-scale structures.

With progressive folding and limb rotation, limbs dip range between 30–55°, and an additional conjugate system of $hk0_b$ shear fractures can be observed (Fig. 6, nets B1 and B2). Earlier stylolites and calcite veins within the limestone beds are curved as they approach their neighbouring strong interlayers or are offset by bed-parallel movements. Bed parallel offset range from few mm to more than 30 cm, and their curvature as they approach the bedding plane indicates a systematic top-to-the-west sense of shear. Limb shortening is commonly expressed by east dipping reverse faults (Fig. 6, nets B1 and B2 and Fig. 7c). SW-dipping back-thrusts displace limbs, which dip more than 50° to the hinterland (Fig. 6, net B2: T_2).

During the final stages of limb rotation, where limbs dip range between 60–85°, ac joints become more pronounced, while $hk0_a$ shear fractures appear to be less prominent. Tightened folds are characterized by a close chevron core, which broadens up-section in an open conjugate box fold (Fig. 7b) forming box lift-off folds (sensu Mitra & Namson 1989). Local stylolitic cleavage of this structural stage forms a small angle or is parallel to the bedding planes (Fig. 7d).

The clusters of shear fracture poles are not perpendicular to the bedding showing similar behaviour to the already described examples of the Rhenohercynian Zone (Fig. 3 nets B2 and C2), which suggest joint rotations due to layer parallel slip.

Short limb deformation

Deformation associated with the progressive rotation of short limbs is characterized by the following joint-pattern: (a) *ac*-joints and $hk0_a$ shear fractures, typical for the long limbs and (b) a new conjugate system of $0kl_c$ shear fractures (Fig. 6, nets D1, D2, E1, E2). The latter system of fractures exhibits multiple sets of slickenlines with the oldest slickenlines showing oblique-slip overprinted by dip-slip extensional movements. Well-developed normal faults in the Skolis and Klokova Anticlines show similar attitude with $0kl_c$ shear fractures and exhibit offsets in the range from centimetres to hundreds of meters (Fig. 6, net E2: N_1 and N_2).

During the initial stages of fold limb rotation, layer-parallel extension is expressed by a set of conjugate normal faults (Fig. 6, net D1 and D2: N_1 and N_2), which have planar geometries and progressively become inactive. During the limb rotation west-dipping normal faults (Fig. 6, net E2: N_2), rotated into a thrust position (Fig. 6, net E2: T_1). In addition m-scale displacements, brecciation and cm-scale arrays of sigmoid en echelon fractures characterize these faults. The kinematics on these en echelon faults suggests that these synthetic faults are hybrid shear fractures. Steepened to the near vertical position the fold limbs are affected by a well-preserved stylolitic cleavage. This newly formed cleavage dips about 60° to 70° to the northeast and transects the bed parallel cleavage, forming a lozenge shaped stylolitic pattern (Fig. 7d).

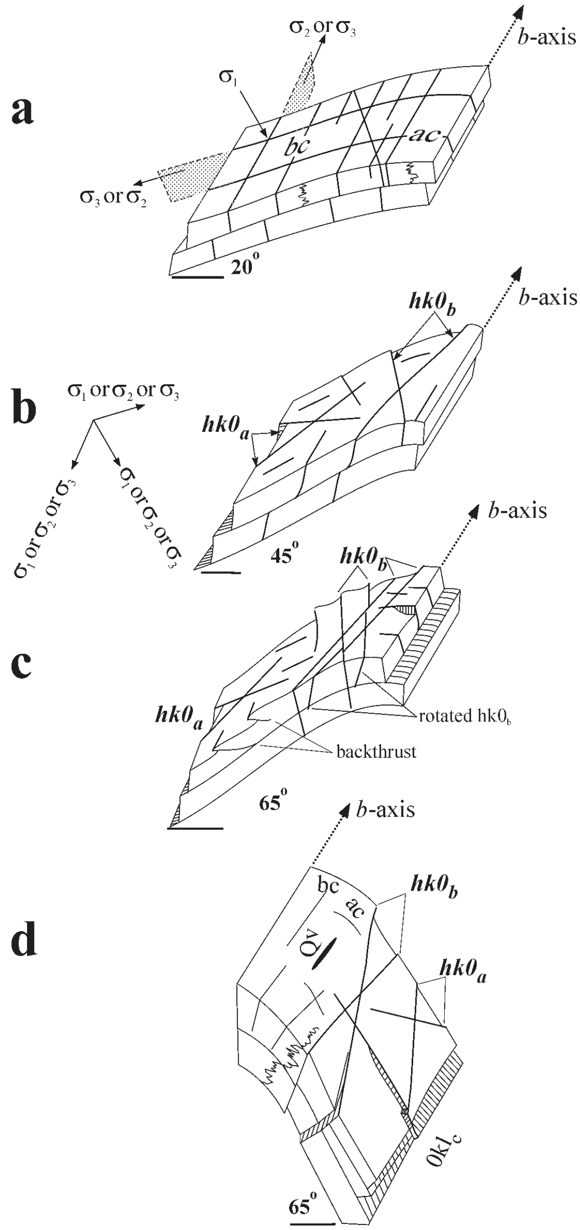

Fig. 8. Summary model showing progressive deformation and associated fractures, the folds are markedly asymmetrical. Fracture labelling in respect to sedimentary layering and fold hinge lines. From top to bottom the first three models correspond to long limbs while the fourth represents the deformation in the short limb.

Synthesis

Our geometric–kinematic analysis reveals that folds in the two fold-and-thrust belts comprise a similar fracture pattern of *ac*, *bc*, hybrid, $hk0_a$ and $hk0_b$ joints.

Stress distribution during fracturing

At the initial stages of folding (Fig. 3, net A2 and Fig. 6, net A2) an orthogonal set of joints (*ac* and *bc*) and hybrid *ac*-, *bc*-joints formed in the long limb, involving approximately synchronous horizontal extension in two directions: parallel and perpendicular to the fold axis (Fig. 8a). In order to interpret this orthogonal set of joints in terms of stress orientation we adopted Hancock's (1985) proposal where: the direction of maximum principal stress σ_1 remains parallel to the intersection direction between the sets, the intermediate σ_2 and the minimum σ_3 principal stresses lie on the joint planes and perpendicular to the σ_1 principal stress axis (Fig. 8a). This mechanism is possible when rapid 90° switching of roughly equal in magnitude σ_2 and σ_3 axes occurs.

For the stress interpretation of shear fractures we used the Navier-Coulomb criterion of failure where the orientation of σ_1 bisects the acute angle formed by the shear fractures. Thus, for the $hk0_a$, the σ_1 axis is parallel to the dip direction of bedding, the σ_2 is perpendicular to the bedding and the σ_3 is parallel to the fold axis (Fig. 8b). The common occurrence $hk0_a$ and $hk0_b$ joints within the same lithological horizon, as well as the formation of these joints in every stage of folding (Figs. 3, 6 and 8) lead us to assume that σ_1, σ_2 and σ_3 changed their magnitudes through the fold evolution. The fluid pressure within the rocks, which changed during folding, could be an important factor controlling the switching of the σ_1, σ_2 and σ_3 axes (see discussion by Price & Cosgrove 1990). The *ac* and associated hybrid joints become abundant as folds amplified (Fig. 3, 6, 8c and d) suggesting an increase of extension parallel to the fold axis. This is supported by volumetric measurements in slates in the southern part of the Rhenohercynian Zone where the stretching rates parallel to the fold axis range up to 15 % (Dittmar et al. 1994).

In the strongly deformed southern parts of the Rhenohercynian Zone in the Taunus where the metamorphism increased reaching the greenschist facies (Meisl 1990) the dominance of $hk0_a$ joints indicates strongly extension parallel to the fold axis. Nevertheless it is important to note that the above described stress distribution is restricted within the layers and can differ from the stress distribution affecting the whole fold-and-thrust belt.

The role of layer parallel shear

Both fold-and-thrust belts of the Rhenohercynian Zone and the external Hellenides have a similar tectonic position as they were underplated beneath earlier oceanic domains, which were destroyed in the central parts of both orogens. The main compressive direction is oriented perpendicular to the structural grain of the belts and is inclined to the stratigraphic discontinuities resulting from the formation of asymmetric folds. The long and short limbs of folds show some differences regarding the formation of fractures (Fig. 8).

The *bc* and associated hybrid joints are abundant within the long limbs and scarce within the short limbs of the folds. This can be explained by the different position of the two limbs in the strain ellipsoid produced by the layer parallel shearing. As the asymmetrical fold initiated, the long limb lay in the extensional field of the strain ellipsoid and *bc* joints changed, whereas the short limb lay in the contractional field of this ellipsoid and *bc* joint formation was hampered.

The prevalence of *ac* and hybrid joints in the short limbs indicates that extension parallel to the fold axis is greater in the short limbs. The presence of $0kl_c$ joints on the short limbs of the folds in the external Hellenides (Fig. 6, net D2 and E2) support this conclusion.

Only in the first stages of folding (Fig. 3, net A1 and Fig. 6, net A1) joints are symmetrically arranged about the dip of layer and hence they can be named according to Hancock's terminology (Fig. 8a and b). As the long limb becomes steeper (Figs. 3 and 6, nets B1 and C1) joints remain steeply dipping and the distribution of poles to fractures do not lie on the *bc* great circle (Fig. 8c). An additional rotation of the joints toward the fold hinge induced by layer parallel shear movements is responsible for this geometrical pattern. In the external Hellenides, where forward movements during folding are pronounced and the deformed rocks are mechanically heterogeneous, joint rotations are stronger (Fig. 6, nets B2 and C2).

Although small joint rotations at the short limb are also observed, they are only of local importance as generally joints within them are symmetrically arranged about the dip of the layers (Figs. 3 and 6, nets D2 and E2).

Furthermore, our analysis indicates local stress distribution within folds that in general differs strongly from the regional stress field controlled by the collision of plates (Zoback & Zoback 1991). Each fracture set studied in this work marks the orientation of a local stress field during the progressive development of fold bend, with an interchange of the principal stress axes.

Conclusions

1. Data from detailed structural analysis of road cuts suggest that the fracture network in the two fold-and-thrust belts show strong similarities. Common fractures are classified as *ac*- *bc*-joints and their hybrids and $hk0_a$, $hk0_b$. Once structures were formed they appear to be continuously active and new fractures of the same attitude were formed during the later stages of deformation.

2. Layer parallel shear and the separation of the succession into different mechanical units is an important mechanism for understanding dispersion of fracture poles over stereonet sectors. In our work the effect of the layer-parallel shear resulted in progressive increase of the angle between the $hk0_a$ and $hk0_b$ shear fractures and the *bc* great circle.

3. Although stress orientation remains constant with respect to the layer, rapid 90° switching of the stress axes are inferred from the coexistence of *ac*-, *bc*-joints and $hk0_a$, $hk0_b$ shear fractures.

4. Extension normal to the dip direction of layering increases during fold tightening.

Acknowledgments: We acknowledge the support of Enterprise Oil Limited, Hellenic Petroleum, M.O.L. and ARCO, Grants No. 18631, 18632. We are also grateful to Prof. W. Meyer who provided helpful comments during 1985 field trips in Rhenohercynian Externides and read parts of this manuscript. Detailed reviews by Dušan Plašienka, and two anonymous referees considerably helped to improve the manuscript and are gratefully acknowledged.

References

Ahrendt H., Clauer N., Hunziker J.C. & Weber K. 1983: Migration of folding and metamorphism in the Rheinische Schiefergebirge deduced from K-Ar and Rb-Sr Age determinations. In: Martin H. & Eder F.W. (Eds.): Intracontinental Fold Belts. *Springer*, Berlin, 323–338.

Auboin J. 1959: Contribution a l'etude geologique de la Grece septentionale: les confins de l'Epire et dela Thessalie. *Ann. Geol. Pays Hellen.* 10, 1–483.

Bernoulli D. & Laubscher H. 1972: The palinspastic problem of the Hellenides. *Eclogae Geol. Helv.* 65, 107–118.

Breddin H. 1956: Die tektonische Deformation der Fossilien im Rheinischen Schiefergebirgen. *Z. Dtsch. Geol. Gesell.* 106, 227–305.

Chester J.S., Logan J.M. & Spang J.H. 1991: Influence of layering and boundary conditions on fault-bend and fault-propagation folding. *Geol. Soc. Amer. Bull.* 103, 1059–1072.

Cloos E. 1961: Bedding slips, wedges, and folding in layered sequences. *Bull. Comm. Géol. Finlande* 33, 106–122.

Cloos H. & Martin H. 1932: Der Gang einer Falte. *Fortschr. Geol. Paläont*. 11, 74–88.

Cooke M.L. & Pollard D.D. 1997: Bedding-plane slip in initial stages of fault-related folding. *J. Struct. Geol.* 19, 567–581.

Couples G.D., Lewis H. & Tanner G. 1998: Strain partitioning during flexural-slip folding. In: Coward M.P., Daltaban T.S. & Johnson H. (Eds): Structural geology in reservoir characterization. *Geol. Soc. Spec. Publ.* 127, 149–165.

Davis G.H. 1984: Structural geology of rocks and regions. *Wiley,* New York.

Degnan P.J. & Robertson A.H.F. 1998: Mesozoic-early Tertiary passive margin evolution of the Pindos ocean (NW Peloponnese, Greece). *Sediment. Geol.* 117, 33–70.

Dennis J.G. 1972: Structural Geology. *Ronald Press,* New York, 1–532.

Dittmar D., Meyer W., Oncken O., Schievenbusch TH., Walter R. & Von Winterfeld C. 1994: Strain partitioning across a fold and thrust belt: the Rheinish Massif, Mid-European Variscides. *J. Struct. Geol.* 16, 1335–1352.

Dittmar U. & Oncken O. 1992: Anatomie und Kinematic eines passiven varistishen Kontinentalrandes — Zum Strukturbau des südwestlichen Rheinishen Schiefergebirges. *Frankfurter Geowiss. Arb.* A11 (TSK IV-Sonderband), 34–37.

Doutsos T. & Prufert J. 1986: Bau und tektonische Entwicklung der Metamorphosen Zone am Taunus-Sudrand (Rheinisches Schiefergebirge). *Geol. Jb. Hessen* 114, 125–149.

Doutsos T., Pe-Piper G., Boronkay K. & Koukouvelas I. 1993: Kinematics of the Central Hellenides. *Tectonics* 12, 936–953.

Doutsos T., Koukouvelas I., Poulimenos G., Kokkalas S., Xypolias P. & Skourlis K. 2000: An exhumation model of the south Peloponnesus, Greece. *Int. J. Earth Sci.* 89, 350–365.

Dunne W.M. & Hancock P.L. 1994: Palaeostress analysis of small-scale brittle structures. In: Hahcock P.L. (Ed.): Continental deformation. *Pergamon Press Ltd*, Oxford, 101–120.

Dunne W.M. 1986: Mesostructural development in detached folds: an example from West Virginia. *J. Geol.* 94, 473–488.

Engelder T. & Geiser P. 1980: On the use of regional joint sets as trajectories of paleostress fields during the development of the Appalachian Plateau, U.S.A. *J. Geophys. Res.* 85, 6319–6341.

Gray M.B. & Mitra G. 1993: Migration of deformation fronts during progressive deformation: evidence from detailed structural studies in the Pennsylvania Anthracite region, USA. *J. Struct. Geol.* 15, 435–449.

Hancock P. 1985: Brittle microtectonics: principles and practice. *J. Struct. Geol.* 7, 437–457.

Hobbs B.E., Means W.D. & Williams P.F. 1976: An outline of structural geology. *Wiley,* New York, 1–571.

Karakitsios V. 1995: The influence of preexisting structure and halokinesis on organic matter preservation and thrust system evolution in the Ionian basin, Northwest Greece. *Amer. Assoc. Petrol. Geol. Bull.* 79, 960–980.

Kisch H.J. 1981: Burial diagenesis in Tertiary 'flysch' of the external zones of the Hellenides in central Greece and the Olympos region, and its tectonic significance. *Eclogae Geol. Helv.* 74, 603–624.

Martin H. & Franke W. 1985: Sonderforschungsbereich 'Entwicklung, Bestand und Eigenschaften der Erdkruste, insbesondere der Geosynklinalraume' (48), Universitat Gottingen: Vom Meeresbecken zum Hochgebirge. In: DFG, Sonderforschungsbereich 1969–84. *VCH Verlagsgesellschaft*, Weinheim, 275–288.

Meyer W. & Stets J. 1980: Zur Palaogeographie von Unter- und Mitteldevon im westlichen und zentralen Rheinischen Sciefergebirge. *Z. Dtsch. Geol. Gesell.* 131, 725–751.

Meyer W., Schulz-Ellermann H.J., Thon B. & Wolf M. 1986: Illit-Kristallinität und Inkohlung in der Sudeifel (Nordflugel der Moselmulde). *Z. Dtsch. Geol. Gesell.* 137, 345–354.

Meisl S. 1990: Metavolcanic rocks in the "Northern Phyllite Zone" at the southern margin of the Rhenohercynian Belt. In: Field Guide 'Mid German Crystalline Rise & Rheinischen Schiefergebirgen'. *Intern. Conf. On Paleozoic Orogens in Central Europe*, 25–42.

Mitra S. & Namson J. 1989: Equal-area balancing. *Amer. J. Sci.* 199, 563–599.

Ohlmacher G.C. & Aydin A. 1995: Progressive deformation and fracture patterns during foreland thrusting in the southern Appalachians. *Amer. J. Sci.* 295, 943–987.

Ohlmacher G.C. & Aydin A. 1997: Mechanics of vein, fault and solution surface formation in the Appalachian Valley and Ridge, northeastern Tennessee, USA: implications for fault friction, state of stress and fluid pressure. *J. Struct. Geol.* 19, 927–944.

Oncken O. 1998: Orogenic mass transfer and reflection seismic patterns-evidence from DEKORP sections across the European Variscides (central Germany). *Tectonophysics* 286, 47–61.

Pe-Piper G. & Koukouvelas I. 1992: Petrology, geochemistry and regional significance of igneous clasts in Parnassos flysch, Amphissa area, Greece. *Neu. Jb. Mineral., Abh.* 164, 94–112.

Plesch A. & Oncken O. 1999: Orogenic wedge growth during collision — constraints on mechanics of a fossil wedge from its kinematic record (Rhenohercynian FTB, Central Europe). *Tectonophysics* 309, 117–139.

Plessmann W. 1966: Losung, Verformung, Transport und Gefuge (Beitrage zur Gesteinsverformung im nordostlichen Rheinischen Schiefergebirge). *Z. Dtsch. Geol. Gesell.* 115, 650–663.

Price N.J. & Cosgrove J.W. 1990: Analysis of geological structures. *Cambridge University Press,* Cambridge, 1–502.

Price N.J. 1967: The tectonic significance of mesoscopic subfabrics in the southern Rocky Mountains of Alberta and British Columbia. *Canad. J. Earth Sci.* 4, 39–70.

Richter D. 1978: The main flysch stages of the Hellenides. In: Closs H., Roeder D. & Schmidt K. (Eds): Alps, Appenines, Hellenides. *Verlagsbuchhandlung,* Stuttgart, 434–438.

Sanderson D.J. 1979: The transition from upright to recumbent folding in the Variscan fold belt of northwest England: a model based on the kinematics of simple shear. *J. Struct. Geol.* 1, 171–180.

Skarmenta J.J. & Price N.J. 1984: Deformation of country rock by an intrusion in the Sierra de Moreno, northern Chilean Andes. *J. Geol. Soc. London*, 141, 901–908.

Smith A.G., Woodcock N.H. & Naylor M.A. 1979: The structural evolution of a Mesozoic continental margin, Othris Mountains, Greece. *J. Geol. Soc. London* 136, 589–603.

Srivastava D.C. & Engelder T. 1990: Crack-propagation sequence and pore-fluid conditions during fault-bend folding in the Appalachian Valley and Ridge, central Pennsylvania. *Geol. Soc. Amer. Bull.* 102, 116–128.

Stearns D.W. 1967: Certain aspects of fracture in naturally deformed rocks. In: Riecker R.E. (Ed.): Rock mechanics seminar. *US Air Force Cambridge Research Laboratories,* Contribution AD669375, 97–118.

Tanner P.W.G. 1989: The flexural-slip mechanism. *J. Struct.*

Geol. 11, 635–655.
Temple P.G. 1968: Mechanics of large-scale gravity sliding in the Greek Peloponnesos. *Geol. Soc. Amer. Bull.* 79, 689–700.
Wunderlich H.G. 1964: Maß, Ablauf und Ursachen orogener Einengung am Beispiel des Rheinischen Schiefergebirges, Ruhrkarbons und Harzes. *Geol. Rdsch.* 54, 861–882.
Xypolias P. & Doutsos T. 2000: Kinematics of rock flow in a crustal-scale shear zone: implication for the orogenic evolution of the southwestern Hellenides. *Geol. Mag.* 137, 81–96.
Xypolias P. & Koukouvelas I. 2001: Kinematic vorticity and strain patterns associated with ductile extrusion in the Chelmos Shear Zone (External Hellenides, Greece). *Tectonophysics* 338, 59–77.
Zoback M.D. & Zoback M.L. 1991: Tectonic stress field of North America and relative plate motions. In: Slemmons D.B., Engdahl E.R., Zoback M.D. & Blackwell D.D. (Eds): Neotectonics of North America. Boulder, Colorado. *Geol. Soc. of America*, Decade Map Vol.1, 339–366.